

## Equipfield line simulation and ion migration prediction for concrete under 2-D electric field

Chih-Chien Liu<sup>1</sup>, Wen-Ten Kuo<sup>\*2</sup> and Chun-Yao Huang<sup>2</sup>

<sup>1</sup>Department of Civil Engineering, ROC Military Academy, No.1, Wei-Wu Rd.,  
Fengshan District, Kaohsiung 83059, Taiwan, R.O.C.

<sup>2</sup>Department of Civil Engineering, National Kaohsiung University of Applied Sciences,  
No. 415, Chien-Kung Rd., Sanmin District, Kaohsiung 80778, Taiwan, R.O.C.

(Received October 17, 2012, Revised February 28, 2013, Accepted May 11, 2013)

**Abstract.** This study attempted to find a proper method applicable to simulating practical equipfield lines of two-dimensional Accelerate Lithium Migration Technique (ALMT), and evaluate the feasibility of using the theoretical ion migration model of one-dimensional ALMT to predict the ion migration behavior of two-dimensional ALMT. The result showed that the electrolyte or carbon plate can be used as matrix to draw equipfield line graph similar to that by using mortar as matrix. Using electrolyte electrode module for simulation has advantages of simple production, easy measurement, rapidness, and economy. The electrolyte module can be used to simulate the equipfield line distribution diagram in practical two-dimensional electrode configuration firstly. Then, several equipfield line zones were marked, and several subzones under one-dimensional ALMT were separated from various equipfield line zones. The theoretical free content distribution of alkali in concrete under two-dimensional electric field effect could be obtained from duration analysis.

**Keywords:** electrochemical; alkali-silica reaction; migration; electrode

### 1. Introduction

The Alkali-Silica Reaction (ASR) is the most extensively distributed alkali aggregate reaction (AAR) type that damages the concrete structures most severely at present (Wang 2010). It occurs after the hydration of cement. The concrete pore solution contains free ions of  $\text{Na}^+$ ,  $\text{K}^+$ ,  $\text{Ca}^{2+}$  and  $\text{OH}^-$ , the  $\text{OH}^-$  breaks the Si-O bonding with lower bond energy on the surface of active aggregate to be combined with positively charged cation into alkali-silica gel. The  $\text{Na}^+$  and  $\text{K}^+$  carry monovalent positive electricity are smaller than  $\text{Ca}^{2+}$ , so they are more likely to be combined into stable alkali-silica gel. The absorption swelling capacity is higher than that of calcium-silica gel, and the concrete will be damaged (Wang 2010). The ASR developed rate in the buildings in hot area is 4-5 times of that in cold zone (Fournier *et al.* 2009). The ASR occurrence probability increases significantly as the temperature rises (Ghanem *et al.* 2010).

The common methods for preventing ASR in fresh concrete include: using low-alkali cement,

---

<sup>\*</sup>Corresponding author, Associate Professor, E-mail: [wtkuo@cc.kuas.edu.tw](mailto:wtkuo@cc.kuas.edu.tw)

using non-reactive aggregate, adding pozzolanic mineral admixture or adding chemical admixture containing Li (Esteves *et al.* 2012, Hasdemir *et al.* 2012, Wang 2010, Bakker 2008). Hobbs (Hobbs 1984) found that when the total alkali content in concrete was lower than  $2 \text{ kg/m}^3$ , the concrete specimen using opal as aggregate would not have expansion reaction. The addition of lithium compound would form lithium-silicon crystal on the reactive aggregate surface, thus reducing the probability of damage resulted from the gel formed with sodium and kalium ions. And then the ASR expansion could thus be inhibited (Feng *et al.* 2010, Bulteel *et al.* 2010). The recommended addition of lithium compound for inhibiting ASR effectively was  $\text{Li}/(\text{Na}+\text{K})$  molar ratio greater than 0.74 (Michael *et al.* 2007).

The most commonly used method for preventing ASR in structures in practice is to prevent water from entering the concrete (Kagimoto and Kawamura 2012). Daidai (Daidai and Torii 2008) indicated that the cracks in the concrete piers of a bridge built in 1972 were filled up with epoxy by waterproofing engineering in 1989, and coated with waterproof layer. However, five years later, the protective layer had obvious cracks, and the bridge was eventually demolished and rebuilt for severe internal damage. Another method is to feed solution containing lithium into concrete to change the concrete properties. The concrete in small thickness can be sprayed with or soaked in lithium solution, but the  $\text{Li}^+$  penetration depth is limited (Folliard *et al.* 2008). If pressurization method is used, the  $\text{Li}^+$  penetration distance is also short, which is time-consuming and produces inconsistent result (Era *et al.* 2008).

The  $\text{Li}^+$  is fed into concrete by applying electric field. The feeding distance can be increased, and the required time can be shortened (Liu *et al.* 2011, Wang *et al.* 2011). The strategy of using Accelerate Lithium Migration Technique (ALMT) to inhibit ASR in concrete is to feed  $\text{Li}^+$  in while removing  $\text{Na}^+$  and  $\text{K}^+$  out of concrete, so as to solve the ASR problem thoroughly (Wang 2010). Fig. 1 shows one-dimensional ALMT electrical module with a constant current density.  $1 \text{ N LiOH} \cdot \text{H}_2\text{O}$  and saturated  $\text{Ca}(\text{OH})_2$  as the anolyte and catholyte, respectively. A #20 304 stainless steel mesh electrode was used to prevent electrode oxidation (Liu 2003); a data logger was utilized to record the voltage variations; an ion chromatograph (IC) was employed to periodically analyze the cation concentration in the catholyte; the temperature change of the cathodic cell was manually measured.

At present, most of studies that use ALMT for repairing ASR discuss the influence of changing the proportioning of concrete, electrode gap, electric field intensity, electrolyte type and degree of deterioration on the migration of  $\text{Na}^+$ ,  $\text{K}^+$  and  $\text{Li}^+$  under the effect of one-dimensional electric field (Wang 2010, Liu *et al.* 2011). The theoretical migration model of ion under electric field effect has been built (Wang 2010). In practice of ALMT, it is predictable that the individual cases handled by one-dimensional electric field directly are limited, so the two-dimensional or three-dimensional space electric field must be used.

This study has two purposes: 1. to find a simple, timesaving and economical method for simulating the equipfield lines of practical application of two-dimensional ALMT; 2. to discuss the feasibility of using the existing theoretical ion migration model of one-dimensional ALMT (Wang *et al.* 2012), in order to predict the ion migration results of application of one-dimensional and two-dimensional ALMT. Several equipfield line zones are marked in the equipfield line direction on the simulated equipfield line distribution diagram firstly. And then several subzones under one-dimensional electric field effect are marked on various equipfield lines. The  $\text{Na}^+$  and  $\text{K}^+$  contents in various subzones at different times are calculated by duration analysis method, and then compared with the content results of test.

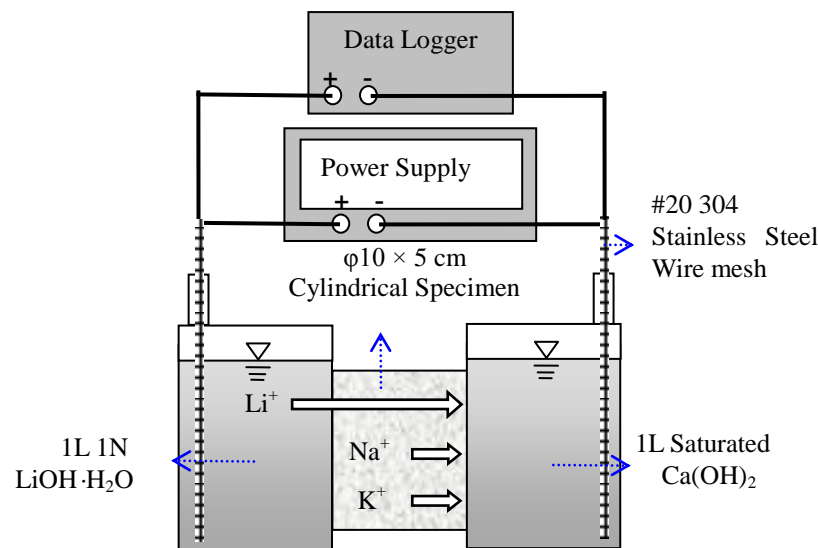


Fig. 1 One-dimensional ALMT electrical module

## 2. Experimental program

### 2.1 Specimen design and electrifying analysis method

This study was divided into two parts. The first part used two different materials as matrix to simulate drawing the equifield line distribution of electrified mortar, which were electrolyte and carbon plate, in order to find a simple and timesaving method to replace concrete which is difficult to be made. The equifield line distributions of different electrode designs were drawn in the practical application of ALMT. The electrode configuration modes were line-to-line and plane-to-plane, as shown in Fig. 2. The distance between electrode centers was designed as 15 cm. The specimen was 15 cm in width and 5 cm in height. The line electrode was designed as circle in diameter of 2.5 cm. The penetration depth was 4 cm, and the line electrode edge was 1.25 cm away from the outer edge of the closest electrode module. A uniform grid in side length of 1.25 cm was marked on the electrode module. When constant voltage was applied, the voltage was recorded and then entered in the surfer 9 program to draw isopotential line and equifield distribution diagrams. The equifield line distribution diagrams of electrode modules made of different material matrices were compared to find out the differences.

The second part produced mortar specimen according to the module measuring equifield line for ALMT electrifying. The mix design of mortar was the same as Wang (Wang 2010). The aggregate-cement ratio was fixed at 2.25 and the aggregate gradation distribution followed ASTM C227. The water-cement ratio was fixed at 0.5. The alkali equivalent in cement was adjusted from 0.52 % Na<sub>2</sub>O<sub>eq</sub> to 2.0% Na<sub>2</sub>O<sub>eq</sub> by adding NaOH. The aggregate was from river sand in the west of Taiwan, and it was metasandstone. The form was removed on the day next to the production of specimen, and then the specimen was cured at 23°C, 100% R.H. for 3 months.

The constant current density applied to line-to-line and plane-to-plane electrode modules was 18 and 9 A/m<sup>2</sup>, respectively, and were electrified for 28 days. The application of 9 A/m<sup>2</sup> to the plane electrode referred to the test in reference (Wang *et al.* 2012), as the surface area of line

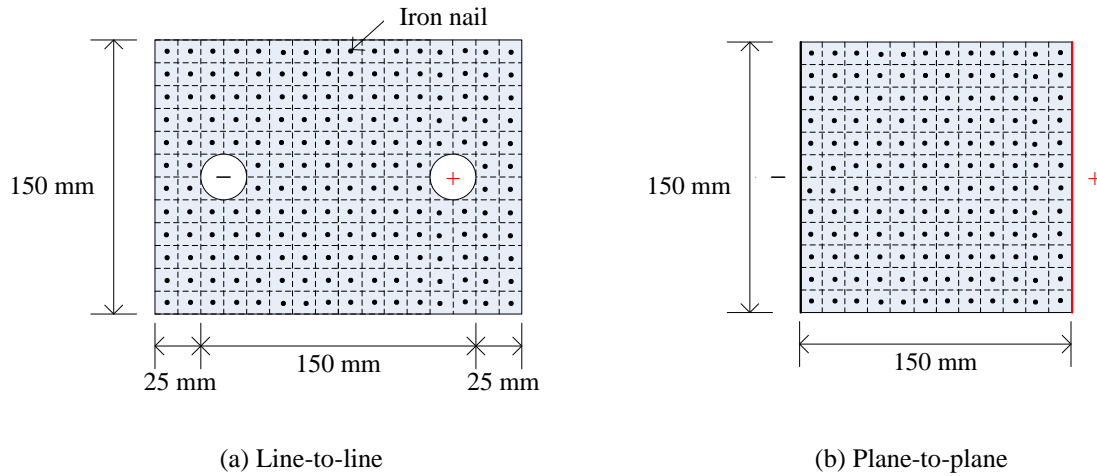


Fig. 2 Electrode configuration modes

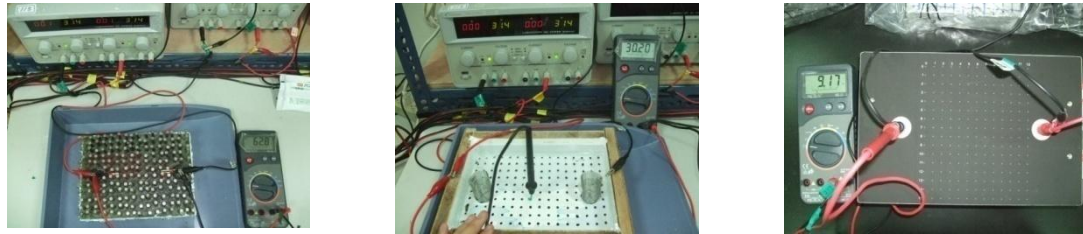
electrode was only half of the plane electrode surface area, in order to apply the same electric quantity in the whole electrifying process. The constant current density of  $18 \text{ A/m}^2$  was applied to the line electrode. The anode used  $1\text{N LiOH}\cdot\text{H}_2\text{O}$  solution, the cathode used saturated  $\text{Ca}(\text{OH})_2$  solution, the stainless steel bar was used as the line electrode, and the stainless steel mesh covered with cotton was used as the plane electrode. As the anodic stainless steel bar had oxidation in the electrifying process, the electrode and solution were renewed once every 7 days.

A cube in side length of 1.25 cm was cut out from the electrified specimen by hand-held cutter, after low-temperature drying and grinding. The free cations in the specimen were dissolved by using water dissolution method referring to AASHTO T260 procedure. The ion chromatograph (IC) was used to analyze the free cation content.

Finally, several equipfield line zones were marked in the equipfield line direction on the two-dimensional electric field in the equipfield line concept by using the developed one-dimensional electric field analysis model (Wang *et al.* 2012). Several sub-active zones of one-dimensional electric field were marked in each equipfield line zone. The free cation content in each one-dimensional electric field sub-zone was used as the initial value, and the duration analysis method was used to calculate the free form content in each one-dimensional electric field sub-zone after the cation shifting out and in per day for each equipfield line zone as the initial value for the analysis on the next day. The calculation proceeded to Day 28. The free cation content distribution in the specimen after 28 days of ALMT electrifying was predicted, and then compared with the test value, so as to evaluate the feasibility of using the equipfield line concept to divide two-dimensional ALMT into one-dimensional electric fields to estimate the ion migration behavior.

## 2.2 Equipfield line drawing method

Take Fig. 2(a) line-to-line electrode module as an example, the power supply applied constant voltage, one end of digital multimeter was connected to the anode, the other end was connected to the iron nail. The iron nail coordinates and voltage difference were recorded. The test photo of the equipfield line drawing for mortar specimen module is shown in Fig. 3(a). The equipfield line



(a) Mortar specimen (b) Electrolyte (c) Carbon matrix modules

Fig. 3 Test photos of the equipfield line

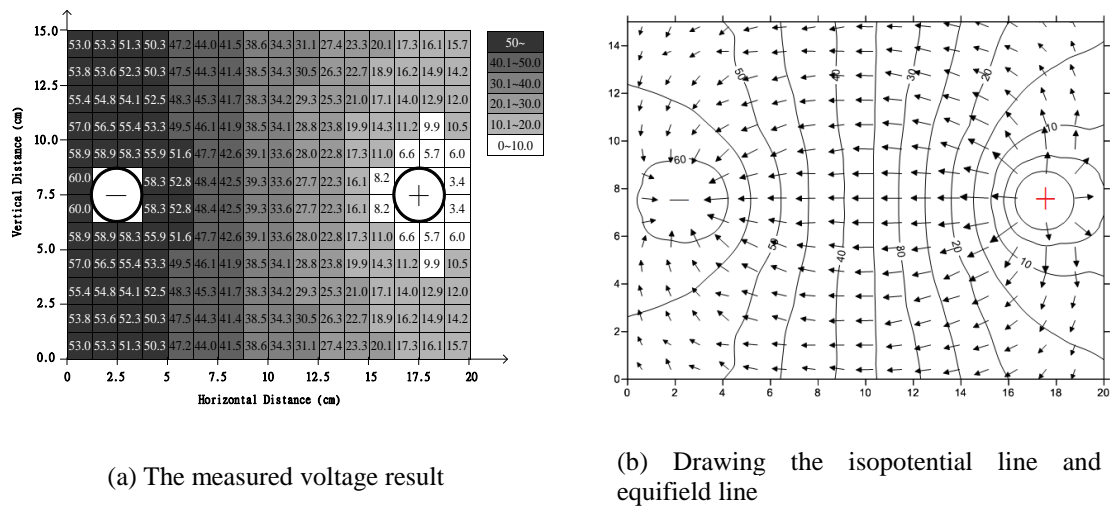


Fig. 4 Description of drawing method of voltage difference and equipfield line of various regions in mortar specimen in water-cement ratio of 0.5

diagram was drawn by using Surfer 9 program according to the results. Take line-to-line electrode as an example, the measured voltage result is shown in Fig. 4(a), Fig. 4(b) shows the isopotential line and equipfield line.

Surfer 9 program is a full-function 3D surface modeling package. The sophisticated interpolation engine transforms the scattered XYZ data into publication-quality maps. Surfer excels at creating contour, vector, shaded relief, image, post, 3D wireframe and 3D surface maps. Surfer is used extensively for terrain modeling, landscape visualization, surface analysis, gridding, volumetrics, 2D map generation, and much, much more.

### 3. Results and discussion

#### 3.1 Feasibility of using electrolyte and carbon plate to simulate mortar electrode module equipfield line distribution

Figs. 3(b) and (c) show the test photos of the equipfield line drawing for electrolyte and carbon

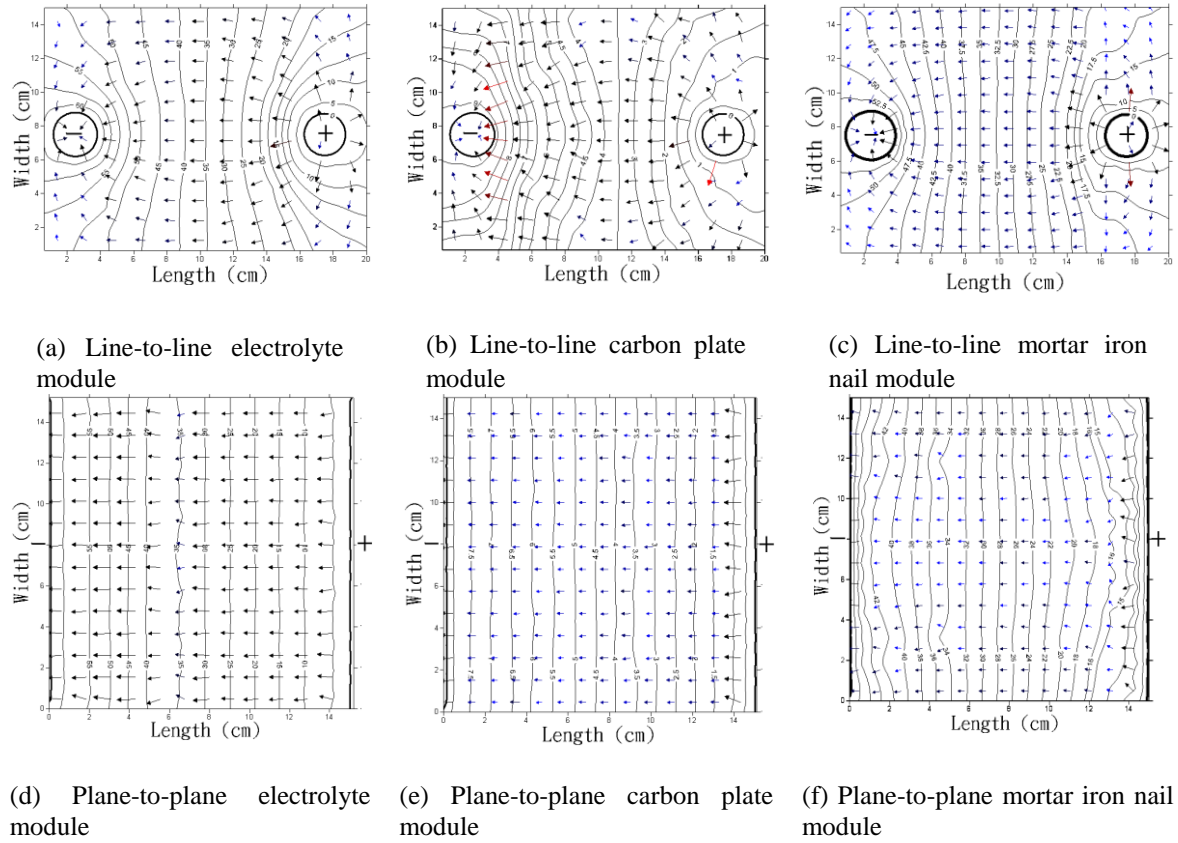


Fig. 5 Electric field distribution diagram

matrix modules, respectively. The drawing steps for the equipotential line of electrolyte and carbon matrix modules are similar to that of mortar specimen module. Fig. 5 shows the equipotential line distribution of matrix of electrolyte, carbon plate and mortar applied with line-to-line and plane-to-plane electric fields respectively. Figs. 5(a) and (d) show the isopotential line and equipotential line diagrams of line-to-line and plane-to-plane electrolyte electrode modules respectively. As the electrolyte has high homogeneity, the diagrams are symmetrical in vertical and horizontal directions. Figs. 5(b) and (e) show the isopotential line and equipotential line diagrams of line-to-line and plane-to-plane carbon plate electrode modules respectively. The shape is similar to that of electrolyte electrode module, however, it is observed in the distribution diagram that some isopotential lines are wavy, indicating that the isopotential line is influenced by the discontinuity of material of carbon plate. Figs. 5(c) and (f) show the isopotential line and equipotential line diagrams of line-to-line and plane-to-plane mortar electrode modules, respectively. If the mortar specimen is compacted uniformly, it can be regarded as homogeneous object. The mortar specimen can be regarded as homogeneous body according to the isopotential line diagram and electric field distribution diagram of mortar specimen. When the anode is plane, the wavy isopotential line may be resulted from inconsistent compaction of contact between the electrode made of stainless steel mesh and the mortar surface.

The first part of this study aimed to find a simple and timesaving to replace concrete which is

difficult to be made, and draw the equifield line distribution of different electrode designs in practical application of ALMT. According to the above discussion, the electrolyte or carbon plate can be used as matrix to draw the electrode module equifield line diagram similar to that of mortar matrix. Using electrolyte electrode module to simulate concrete electrode module to draw equifield line diagram has the advantages of simple production, easy measurement of voltage, rapidness and economy. Thus, it is applicable to drawing practically simulated equifield line before practical application of ALMT to solving ASR problem, so as to assist in calculating and estimating the probable results of ion migration before practical implementation.

### 3.2 Use theoretical value of one-dimensional electric field ion migration to predict ion migration of plane-to-plane electrode module

Wang *et al.* (2012) studied the mortar specimen with the same mix proportion and curing condition as in this study. In the empirical equation of ion migration under one-dimensional electric field effect, the one-dimensional electric field test uses mortar cylinder specimen with section in diameter of 10 cm and in height of 5-20 cm. It is found that the velocity of removing  $\text{Na}^+$  and  $\text{K}^+$  related to ASR out of the specimen is proportional to the constant current density. The  $\text{Na}^+$  removal velocity is  $0.019i$  ( $\times 10^{-3}$  mole/h),  $\text{K}^+$  removal velocity is  $0.0048i$  ( $\times 10^{-3}$  mole/h), and  $i$  is the current density ( $\text{A/m}^2$ ).

The plane-to-plane electrified module is designed to be applied with  $9 \text{ A/m}^2$  constant current density in this study. As the power on area of empirical equation adopts circular cross-section area in diameter of 10 cm, it must be converted into average cross-section area of each specimen cube as actual removal velocity of ions. Since the cross-section area of each subzone in Fig. 6(b) is  $0.000625 \text{ m}^2$ . The  $\text{Na}^+$  and  $\text{K}^+$  removal velocity in each subzone is  $3.37 \times 10^{-4}$  mole/day and  $0.85 \times 10^{-4}$  mole/day, respectively.

The second part of this study discussed the feasibility of using the equifield line concept to divide two-dimensional ALMT into one-dimensional electric fields to estimate the ion migration behavior. First, the plane-to-plane electrified module under the same one-dimensional electric field

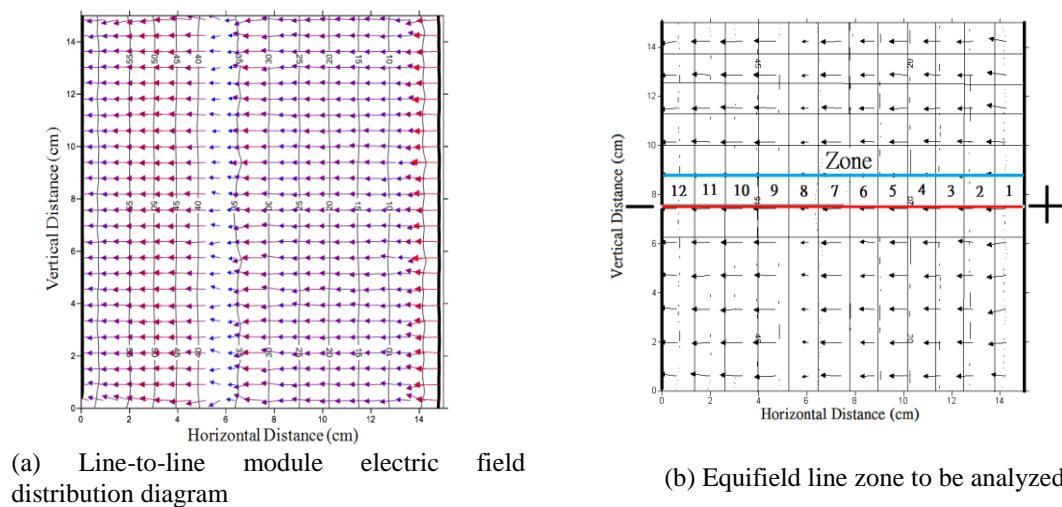


Fig. 6 Plane-to-plane electrode module



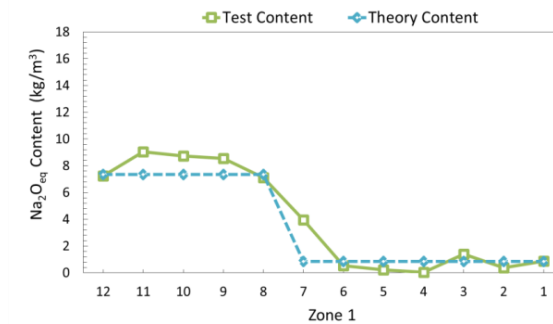


Fig. 7 Comparison between theoretical predicted value and test result of free  $\text{Na}_2\text{O}_{\text{eq}}$  content in Zone 1 of plane-to-plane electrode module

effect was analyzed, as shown in Fig. 6. The electrolyte electrode module was used to draw isopotential line and equipfield line distribution diagrams. Uniform grids in side length of 1.25 cm were marked on the module plane, and 12 equipfield line zones were marked on the plane electrode. The equipfield line zone (Zone 1) above the symmetry axis of electrode connection was analyzed. The equipfield line zone was divided into 12 subzones, and each subzone was under the effect of one-dimensional electric field.

As limited to the  $\text{Li}^+$  content measuring means, IC was used for analysis in this study. Therefore, only the free ion content obtained from water dissolution was measured, in order to compare the estimated theoretical value of ion of two-dimensional ALMT with the test value. The free form content of alkali metal ions inside mortar specimen in the pore solution was analyzed first. It was found that the free  $\text{Na}^+$  and  $\text{K}^+$  contents accounted for 60-80% of total contents of  $\text{Na}^+$  and  $\text{K}^+$ , respectively.

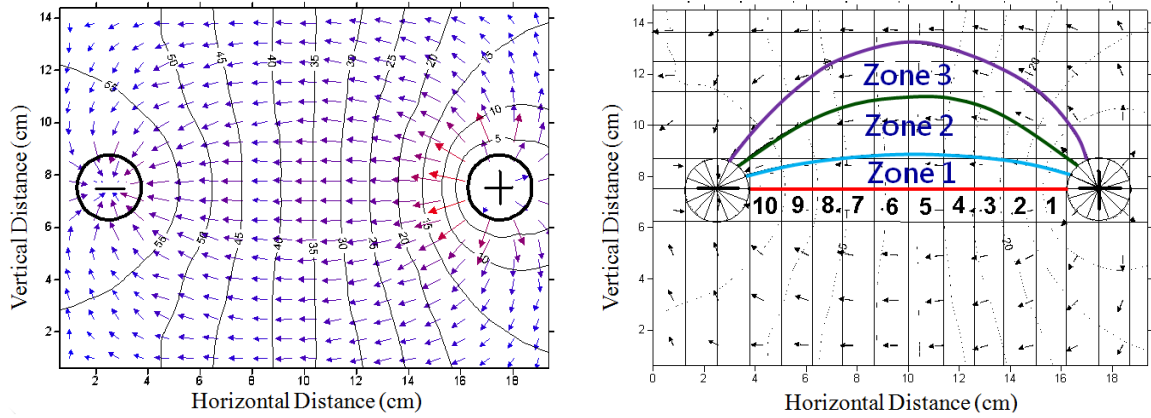
The empirical equation of one-dimensional cation migration was used to calculate the total content of initial free  $\text{Na}^+$  and  $\text{K}^+$  in each subzone. One day was a duration computing unit. The amount of movement of  $\text{Na}^+$  and  $\text{K}^+$  in initial mortar specimen on Day 1 could be calculated by the given electric field intensity, and the initial amount in each subzone at the beginning of electrifying on Day 2 was obtained. Then, the amount of movement on Day 2 could be calculated, and the initial amount on Day 3 was obtained, and so forth. The theoretical free  $\text{Na}^+$  and  $\text{K}^+$  content in the mortar specimen on Day 28 of electrifying could be obtained.

Fig. 7 compares the prediction and test results of theoretical value of free  $\text{Na}_2\text{O}_{\text{eq}}$  content in Zone 1 of mortar specimen in water-cement ratio of 0.5 using plane-to-plane electrode module. It was found that there was no significant difference between the predicted free  $\text{Na}_2\text{O}_{\text{eq}}$  content and test value, suggesting that the empirical equation of one-dimensional electric field ion migration of Wang (Wang 2010) could be used to predict the cation migration under one-dimensional electric field effect in large sized mortar blocks.

### 3.3 Use theoretical value of one-dimensional electric field ion migration to predict ion migration of line-to-line electrode module

The line-to-line electrified module is shown in Fig. 8. The electrolyte electrode module was used to draw isopotential line and equipfield line distribution diagrams. Uniform grids in side length

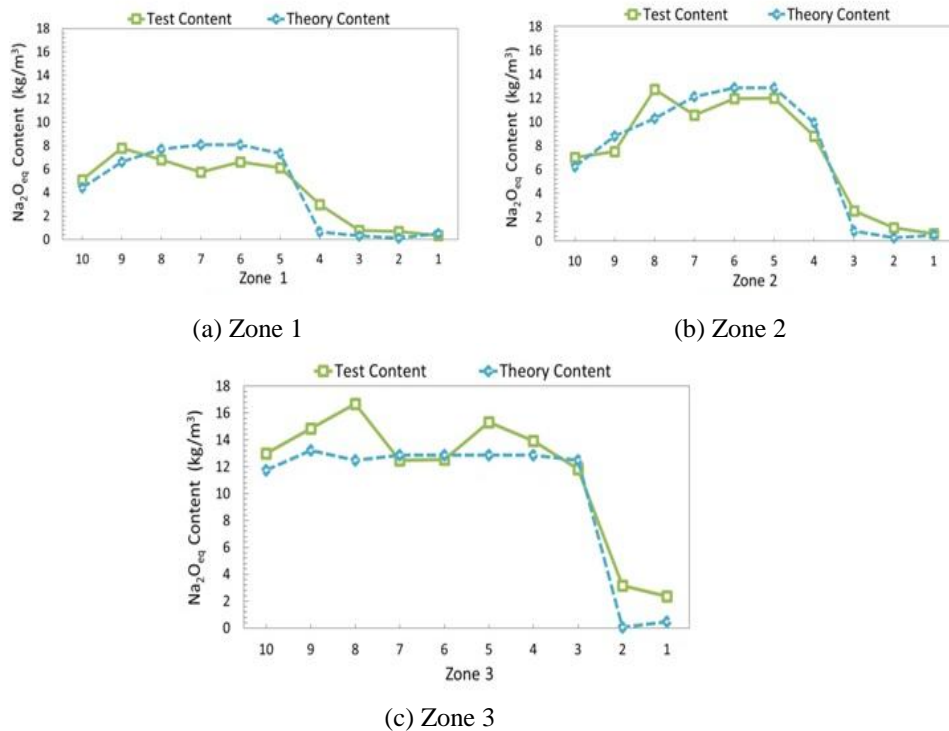




(a) Line-to-line module electric field distribution diagram

(b) 3 equipfield line zones to be analyzed

Fig. 8 Line-to-line electrode module



(a) Zone 1

(b) Zone 2

(c) Zone 3

Fig. 9 Comparison between prediction and test results of theoretical value of residual free  $\text{Na}_2\text{O}_{\text{eq}}$  content in Zone 1-3 of line-to-line electrode module

of 1.25 cm were marked on the module plane, and the periphery of line electrode was equally divided into 16 parts. The three equipfield line zones (Zone 1-3) connected to symmetry axis of electrode connection were analyzed. Each equipfield line zone was divided into 10 subzones, and

each subzone was under the effect of one-dimensional electric field.

The line-to-line electrified module was applied with  $18 \text{ A/m}^2$  constant current density in this study. The anode and cathode were in diameter of 2.5 cm, in depth of 4 cm, and the lateral surface area was  $0.002944 \text{ m}^2$ . The applied rated current was 0.053 A, which was equally divided into 16 parts. The rated magnitude of current distributed to each part was 0.0033 A, namely, the current passing through Zone in Fig. 8(b) was 0.0033 A. The passed magnitude of current was divided by the average cross-section area of grids to obtain the average current density, and the original  $\text{Na}^+$  and  $\text{K}^+$  contents in the mortar specimen in each subzone in Fig. 8(b) were calculated.

As the power on area of empirical equation was circular cross-section area in diameter of 10 cm, it was converted into average sectional area of each specimen cube, in order to determine the actual removal velocity of ions. It was found that in the same electric field line, the current was identical, and the cross-section areas were different. Thus, the current densities were different, but the ion removal velocity was the same. The  $\text{Na}^+$  removal velocity in each subzone was  $1.92 \times 10^{-4}$  mole/day, and the  $\text{K}^+$  removal velocity was  $0.49 \times 10^{-4}$  mole/day.

Artificial intelligence methods based on machine learning has been used to develop rules for automatic categorization of concrete quality. The rapid chloride permeability test - Nordtest Method BUILD 492 method was used for determining chloride ions penetration in concrete. Performed experimental tests on obtained chloride migration provided data for learning and testing of rules discovered by machine learning techniques (Marks *et al.* 2012). In this research, the theoretical ion migration model of one-dimensional ALMT (Wang 2010) was used as the input data of ions migration velocity under electrified application.

Figs. 9(a)-(c) compare the prediction and test results of theoretical value of free  $\text{Na}_2\text{O}_{\text{eq}}$  content in Zone 1-3 of mortar specimen in water-cement ratio of 0.5 using line-to-line electrode module. It was found that there was no significant difference between the predicted  $\text{Na}_2\text{O}_{\text{eq}}$  content and test value in each equipfield line zone in Zone 1 with the maximum electric field intensity or in Zone 3 with lower electric field intensity. In other words, the two-dimensional electric field ALMT test could use the concept of equipfield line to divide two-dimensional electric field into different equipfield line active zones. For each equipfield line active zone, the theoretical model of ion migration obtained from one-dimensional ALMT test was used to predict the result of ion migration using duration analysis method.

According to the analytic results in Sections 3.2 and 3.3, the empirical equation of one-dimensional electric field ion migration in literatures could be used to predict the ion migration behavior under one-dimensional and two-dimensional electric field effects in practical application of ALMT, thus facilitating practical design of ALMT. According to the results of this study, the electrolyte module can be used to simulate the isopotential line and equipfield line distribution diagrams in practical two-dimensional electrode configuration before practical application of ALMT. Several equipfield line zones are marked in equipfield line direction, and each equipfield line zone is divided into several subzones under one-dimensional electric field effect. The empirical equation of cation migration under one-dimensional electric field effect is used to calculate total content of initial free  $\text{Na}^+$  and  $\text{K}^+$  in each subzone. The required time interval is selected as a duration computing unit. The amount of movement of  $\text{Na}^+$  and  $\text{K}^+$  in the initial mortar specimen in the first duration can be calculated by the known electric field intensity as the initial amount in each subzone before the electrifying in the second duration. The amount of movement in the second duration is calculated, and the initial amount before electrifying in the third duration can be obtained. The theoretical free  $\text{Na}^+$  and  $\text{K}^+$  contents in the concrete in the design power on time can be obtained.

#### 4. Conclusions

Based on the results, the following conclusions are obtained:

- The electrolyte or carbon plate matrix can be used to draw electrode module equipfield line diagram similar to that of mortar matrix, and the simulation using electrolyte electrode module has advantages of simple production, easy measurement of voltage, rapidness and economy. Thus, it is applicable to drawing equipfield line before practical application of ALMT to solving ASR problem.
- The empirical equation of one-dimensional electric field ion migration can be used to predict the ion migration behavior under one-dimensional and two-dimensional electric field effects in practical application of ALMT. The electrolyte module is used to simulate the equipfield line distribution diagram in practical two-dimensional electrode configuration. Several equipfield line zones are marked in equipfield line direction, and each equipfield line zone is divided into several subzones under one-dimensional electric field effect. The total content of initial free  $\text{Na}^+$  and  $\text{K}^+$  in each subzone is calculated first, and the required time interval is selected as one duration computing unit by using the empirical equation of cation migration under one-dimensional electric field effect. The known electric field intensity is used to calculate the amount of movement of  $\text{Na}^+$  and  $\text{K}^+$  in the initial mortar specimen in the first duration as the initial amount in each subzone before electrifying in the second duration. The theoretical free  $\text{Na}^+$  and  $\text{K}^+$  content distribution in the concrete under two-dimensional electric field effect can be obtained.

#### Acknowledgements

The authors would like to thank the National Science Council of Taiwan for their financial support of this research under Contract No. NSC 100-2221-E-145-006.

#### References

- Bakker, J.D. (2008), "Control of ASR related risks in the Netherlands", *Proceedings of the 13th International Conference on Alkali-Aggregate Reaction in Concrete*, Trondheim, Norway, June.
- Bulteel, D., Garcia-Diaz, E. and Degrugilliers, P. (2010), "Influence of lithium hydroxide on alkali-silica reaction", *Cem. Concr. Res.*, **40**(4), 526-530.
- Daidai, T. and Torii, K. (2008), "A proposal for rehabilitation of ASR-affected bridge piers with fractured steel bars", *Proceeding of the 13th International Conference on Alkali-Aggregate Reaction*, Trondheim, Norway, June.
- Era, K., Mihara, T., Kaneyoshi, A. and Miyagawa, T. (2008), "Controlling effect of lithium nitrite on alkali-aggregate reaction", *Proceeding of the 13th International Conference on Alkali-Aggregate Reaction*, Trondheim, Norway, June.
- Esteves, T.C., Rajamma, R., Soares, D., Silva, A.S., Ferreira, V.M. and Labrincha, J.A. (2012), "Use of biomass fly ash for mitigation of alkali-silica reaction of cement mortars", *Constr. Build. Mater.*, **26**(1), 687-693.
- Feng, X., Thomas, M.D.A., Bremner, T.W., Folliard, K.J. and Fournier, B. (2010), "New observations on the mechanism of lithium nitrate against alkali silica reaction (ASR)", *Cem. Concr. Res.*, **40**(1), 94-101.
- Folliard, K.J., Thomas, M.D.A., Ideker, J.H., East, B. and Fournier, B. (2008), "Case studies of treating ASR-affected structures with lithium nitrate", *Proceeding of the 13th International Conference on Alkali-*

- Aggregate Reaction*, Trondheim, Norway, June.
- Fournier, B., Ideker, J.H., Folliard, K.J. and Thomas, M.D.A. (2009), "Effect of environmental conditions on expansion in concrete due to alkali-silica reaction (ASR)", *Mater. Charact.*, **60**(7), 669-679.
- Ghanem, H., Zollinger, D. and Lytton, R. (2010), "Predicting ASR aggregate reactivity in terms of its activation energy", *Constr. Build. Mater.*, **24**(7), 1101-1108.
- Hasdemir, S., Tugrul, A. and Yilmaz, M. (2012), "Evaluation of alkali reactivity of natural sands", *Constr. Build. Mater.*, **29**, 378-385.
- Hobbs, D.W. (1984), "Expansion of concrete due to alkali-silica reaction", *Struct. Eng.*, **62a**(1), 26-33.
- Kagimoto, H. and Kawamura, M. (2011), "Measurements of strain and humidity within massive concrete cylinders related to the formation of ASR surface cracks", *Cem. Concr. Res.*, **41**(8), 808-816.
- Liu, C.C., Lee, C. and Wang, W.C. (2011), "Behavior of cations in mortar under accelerated lithium migration technique controlled by a constant voltage", *J. Mar. Sci. Technol.*, **19**(1), 26-34.
- Marks, M., Jozwiak-Niedzwiedzka, D. and Glinicki, M.A. (2012), "Automatic categorization of chloride migration into concrete modified with CFBC ash", *Comput. Concrete*, **9**(5), 393-405.
- Michael, D.A., Thomas, B.F., Kevin, J.F., Jason, H.I. and Yadhira, R. (2007), "The use of lithium to prevent or mitigate alkali-silica reaction in concrete pavements and structures", Federal Highway Administration, U.S. Department Transportation, FHWA-HRT-06-133, 29-31.
- Wang, W.C. (2010), "A study of using one dimensional electrochemical cation migration technique to inhibit concrete ASR", Ph.D. Dissertation, National Central University, Jhongli. (in Chinese).
- Wang, W.C., Liu, C.C. and Lee, C. (2011), "Migration of cations in mortar under an electrical field controlled by a constant current density", *Adv. Mater. Res.*, **150-151**, 362-372.
- Wang, W.C., Liu, C.C. and Lee, C. (2012), "Effective ASR inhibiting length and applied electrical field under accelerated lithium migration technique", *J. Mar. Sci. Technol.*, **20**(3), 245-252.